Physics with an e^+e^- Linear Collider at High Luminosity

P.M. Zerwas
Deutsches Elektronen–Synchrotron DESY
D–22603 Hamburg, FRG

Abstract

The physics potential is summarized briefly for an e^+e^- linear collider operating at center–of–mass energies up to $\sqrt{s} = 1$ TeV and at integrated luminosities up to $\int \mathcal{L} = 0.5$ ab^{-1} per year. This machine will allow to perform precision studies of the top quark and the electroweak gauge bosons at the per–mille level. It will be an ideal instrument to investigate the properties of the Higgs boson and to establish essential elements of the Higgs mechanism *sui generis*. In the area beyond the Standard Model, new particles and their interactions can be explored comprehensively. In supersymmetric theories, the mechanism of the symmetry breaking can be investigated experimentally and the underlying unified theory can be reconstructed eventually at a scale near the Planck scale. Such an e^+e^- linear collider provides unique opportunities in areas complementary to the LHC, and the high precision allows stable extrapolations up to scales near the Planck scale.

1 Synopsis

The knowledge of the fundamental constituents of matter and their interactions has been greatly advanced in the past three decades by operating e^+e^- colliders. A coherent picture of the structure of matter has emerged, that is adequately described by the Standard Model, in many of its facets at a level of unprecedented accuracy. However, the Standard Model does not provide us with a comprehensive theory of matter. Neither the fundamental parameters, masses and couplings, nor the symmetry pattern can be explained, but they are merely built into the model. Moreover, gravity is not incorporated at the quantum level. First steps to solutions of these problems are associated with the unification of the electroweak and the strong forces, and with the supersymmetric extension of the model which provides a bridge from the presently explored energy scales up to scales close to the Planck mass.

Two strategies can be followed to enter into the area beyond the Standard Model. (*i*) Properties of the particles and forces within the Standard Model will be affected by new energy scales. Precision studies of the top quark, the electroweak gauge bosons and the Higgs boson can thus reveal clues to the physics beyond the Standard Model. (*ii*) Above the mass thresholds, new phenomena can be searched for directly and studied thoroughly so that the underlying basic theories can be reconstructed.

In this dual picture a variety of fundamental problems still remain to be solved within the Standard Model [1, 2], demanding experiments at energies beyond the range of existing accelerators.
(*i*) The mass of the *top quark* is much larger than the masses of the electroweak gauge bosons. Understanding the rôle of this particle in Nature is therefore an important goal for the future. In the $t\bar{t}$ threshold region of e^+e^- collisions the top quark mass can be measured to an accuracy better than 200 MeV. This is a desirable goal since future theories of flavor dynamics should provide relations among the lepton/quark masses and mixing angles in which the heavy top quark is expected to play a key rôle. In addition, stringent tests in the electroweak and Higgs sector of the Standard Model can be carried out when the top mass is known very accurately. Helicity analyses of the $t\bar{t}$ production vertex and the t decay vertex will determine the magnetic dipole moments of the top quark and the chirality of the (tb) decay current at the per–cent level. Bounds on the CP violating electric dipole moments of the t quark can be set to 10^{-18} e cm.
(*ii*) Studying the dynamics of the *electroweak gauge bosons* is another important task at high energy e^+e^- colliders. The form and the strength of the triple and quartic couplings of these particles are

uniquely predicted by the non–abelian gauge symmetry of the theory, defining the electroweak charges, the magnetic dipole moments and the electric quadrupole moments of the $W^{\pm}$ bosons in the static limit. Tests of the fundamental symmetry concepts can be performed at an accuracy of 10^{-3} down to 10^{-4}.
(*iii*) A high–luminosity e^+e^- collider with an energy between 300 and 500 GeV will be an ideal instrument to search for *Higgs particles* [3] throughout the mass range characterized by the scale of electroweak symmetry breaking, and to investigate their properties. The intermediate Higgs mass range below ~ 200 GeV is the theoretically and experimentally preferred region. In this scenario Higgs particles remain weakly interacting up to the scale of grand unification, thus providing a basis for the renormalization of the electroweak mixing angle $\sin^2\theta_W$ from the GUT symmetry value 3/8 down to the experimentally observed value close to 0.2. Once the Higgs particle is found, its properties can be studied thoroughly, the external quantum numbers $\mathcal{J}^{\mathcal{PC}}$ and the Higgs couplings, including the self–couplings of the particle. The measurements of these couplings are the necessary ingredient to establish the Higgs mechanism *sui generis* experimentally.

Even though many facets of the Standard Model are experimentally supported at a level of very high accuracy, extensions should nevertheless be anticipated as argued before. The next generation of accelerators can shed light on three domains in the area beyond the Standard Model.

The Grand Unification of the gauge symmetries [4] suggests itself quite naturally. This idea can be realized in different scenarios some of which predict new vector bosons and a plethora of new fermions. Mass scales of these novel particles could be as low as a few hundred GeV.

A very important theoretical extension of the Standard Model, which is interrelated with the unification of the gauge symmetries, is Supersymmetry [5]. This novel symmetry concept unifies matter and forces by pairing the associated fermionic and bosonic particles in novel multiplets. Several arguments strongly support the hypothesis that this symmetry is realized in Nature. (*i*) Supersymmetry stabilizes light masses of Higgs particles in the context of very high energy scales as demanded by grand unified theories. (*ii*) Supersymmetry may generate the Higgs mechanism itself by inducing the radiative symmetry breaking of $SU(2)_L \times U(1)_Y$ while leaving $U(1)_{EM}$ and $SU(3)_c$ unbroken for a top quark mass between 150 and 200 GeV. (*iii*) This symmetry picture is also strongly supported by the successful prediction of the electroweak mixing angle in the minimal version of the theory. The particle spectrum in this theory drives the evolution of the electroweak mixing angle from the GUT value 3/8 down to $\sin^2\theta_W = 0.2336 \pm 0.0017$ which is within a margin of ~ 0.002 to the experimental value $\sin^2\theta_W^{exp} = 0.2316 \pm 0.0002$.

In supersymmetric theories a spectrum of several neutral and charged Higgs bosons is predicted. The mass of the lightest Higgs boson is in nearly all scenarios less than ~ 150 GeV while the heavy Higgs particles have masses of the order of the electroweak symmetry breaking scale. Many other novel particles are predicted in supersymmetric theories. The scalar partners of the leptons could have masses in the range of ~ 200 GeV whereas squarks are expected to be considerably heavier. The lightest supersymmetric states are likely to be non–colored gaugino/higgsino states with masses possibly in the 100 GeV range. Searching for these supersymmetric particles will be one of the most important tasks at future e^+e^- colliders. Moreover, the high accuracy which can be achieved when masses and couplings are measured, will allow us to determine the mechanism of supersymmetry breaking and to extrapolate the basic parameters of the theory so that the key elements of the underlying grand unified theories at scales potentially close to the Planck scale can be reconstructed.

While new high–mass vector bosons and particles carrying color quantum numbers can be searched for very efficiently at hadron colliders, e^+e^- colliders provide in many ways unique opportunities to discover and explore non–colored particles. This is most obvious in supersymmetric theories. Combining LEP2 analyses with future searches at the Tevatron and the LHC, the light and heavy Higgs bosons can individually be found only in part of the supersymmetry parameter space. Squarks and gluinos can be searched for very efficiently at the LHC. Yet precision studies of their properties are possible only in part of the parameter space. Similarly non-colored supersymmetric particles; a model–independent conclusive analysis of gauginos/higgsinos and scalar sleptons can only be carried out at e^+e^- colliders with well–defined kinematics at the level of the subprocesses. The detailed knowledge of all the properties of the colored and non–colored supersymmetric states will enable us to reveal the mechanism of supersymmetry breaking and the structure of the underlying theory.

Thus, the physics progamme of e^+e^- linear colliders is in many aspects complementary to the programme of the pp collider LHC. The high accuracy which can be achieved at e^+e^- colliders in exploring the properties of the top quark, electroweak gauge bosons, Higgs particles and supersymmetric particles will enable us to cover the energy range above the existing machines up to the TeV region in a conclusive form, eventually providing us with essential clues to the basic structure of matter and of the laws of physics.

The discussion will focus on the physics program at an e^+e^- linear collider operating at center–of–mass energies above LEP2 up to about 1 TeV. Primarily the potential high–luminosity runs, collecting integrated luminosities up to $0.5\,\mathrm{ab}^{-1}$ *per annum* will be described. Also the results expected from high–luminosity runs at low energies on the Z resonance, the GigaZ mode, and near the WW threshold will be summarized. Electrons and positrons will in general be assumed polarized to 80% and 60%, respectively. Specific problems which can be solved in eγ and $\gamma\gamma$ modes of the linear collider will be addressed in the appropriate context.

This summary report is built on the general linear collider review Ref.[6]. Other material can be found in Refs.[7], experimental aspects in particular in Ref.[8]. For recent summaries of LHC physics and $\mu\mu$ physics see Refs.[9] and [10], respectively.

2 Top Quark Physics

Top quarks are the heaviest matter particles in the 3–family Standard Model. Introduced to incorporate CP violation in the left–handed charged current sector, they may therefore hold the key for aspects of the physics beyond the Standard Model at high–energy scales. Examples in which the large t mass is crucial, are multi–Higgs doublet models, models of dynamical symmetry breaking, compositeness and supersymmetry. Strong indirect evidence for the existence of top quarks, based on the well established gauge symmetry pattern of the Standard Model, had been accumulated quite early. By evaluating the high–precision electroweak data, the value of the top quark mass was estimated to be $m_t = 180 \pm 14$ GeV. Top quarks have recently been observed directly by the two Tevatron experiments [11], corresponding to a mass of $m_t = 173.8 \pm 5.2$ GeV which is in striking agreement with the result of the electroweak analysis.

2.1 Profile of the Top Quark

For a top mass larger than the W mass, the channel

$$t \to b + W^+$$

is the dominant decay mode. For $\mathrm{m}_t \sim 175\,\mathrm{GeV}$ the width of the top quark, $\Gamma_t \sim 1.4\,\mathrm{GeV}$, is so large compared with the scale Λ of the strong interactions that this quark can be treated as a bare quantum which is not dressed by non–pertubative strong interactions [12].

Chirality of the (tb) decay current: The precise determination of the weak isospin quantum numbers does not allow for large deviations of the (tb) decay current from the left–handed SM prescription. Nevertheless, since $V + A$ admixtures may grow with the masses of the quarks involved [through mixing with heavy mirror quarks, for instance], it is necessary to check the chirality of the decay current directly. The l^+ energy distribution in the semileptonic decay chain $t \to W^+ \to l^+$ depends on the chirality of the current. Any deviation from the standard $V - A$ current would lead to a stiffening of the spectrum and, in particular, to a non-zero value at the upper end–point of the energy distribution. A sensitivity of about 5% to a possible $V + A$ admixture can be reached experimentally [13].

Non–standard top decays could occur in supersymmetric extensions of the Standard Model: top decays into charged Higgs bosons and/or top decays to stop particles, $t \to b + H^+$ and $t \to \tilde{t} + \tilde{\chi}^o_1$. If kinematically allowed, branching ratios of order 10% are expected in both cases so that these decay modes could be observed easily. Decays with signatures as clean as $t \to c\gamma, cZ$ may be detected for branching ratios of order 10^{-4} and less.

The main production mechanism for top quarks in e^+e^- collisions is the annihilation channel [14],

$$e^+e^- \stackrel{\gamma,Z}{\longrightarrow} t\bar{t}$$

For $m_t \sim 175$ GeV, the maximum of the cross section $\sigma(t\bar{t}) \sim 800$ fb is reached about 30 GeV above the threshold, giving rise to a million top quarks in two years of collider operation. If the scale of new areas beyond the Standard Model is much larger than the collider energy, the electroweak production currents can globally be described by form factors which reduce to anomalous Z charges, anomalous magnetic dipole moments and electric dipole moments.

Magnetic dipole moments: If the electrons in $e^+e^- \to t\bar{t}$ are left–handedly polarized, the top quarks are produced preferentially as left–handed particles in the forward direction while only a small fraction is produced as right–handed particles in the backward direction [15], so that the backward direction is most sensitive to small anomalous magnetic moments of the top quarks. The anomalous magnetic moments can be bounded to the percent level by measuring the angular dependence of the t quark cross section in this region.

Electric dipole moments: These moments are generated by CP–non invariant interactions. Non–zero values of the moments can be detected through non–vanishing expectation values of CP–odd momentum tensors such as $T_{ij} = (q_+ - q_-)_i (q_+ \times q_-)_j$ with $q_\pm$ being unit momentum vectors of the W decay leptons. Sensitivity limits to γ, Z electric dipole moments of $\lesssim 10^{-18}$ e cm can be reached [16] for an integrated luminosity of $\int \mathcal{L} = 100$ fb^{-1} at $\sqrt{s} = 500$ GeV.

2.2 The Top Mass

Quark–antiquark production near the threshold in e^+e^- collisions is of exceptional interest. The long time which the particles stay close together at low velocities, allows the strong interactions to build up rich structures of bound states and resonances. This picture would have applied to top quarks up to the mass range of ~ 130 GeV. Beyond this value, the picture changes quite dramatically as a result of the rapid top decay: The decay time of the states becomes shorter than the revolution time of the constituents so that toponium resonances cannot be formed any more [12]. For a while, however, remnants of the $1S$ state give rise to a peak in the excitation curve, yet it disappears for t masses in excess of 180 GeV. Nevertheless, across this range the resonance remnants induce a steep rise of the cross section near the threshold.

Since the rapid t decay restricts the interaction region to small distances, the excitation curve can be predicted in perturbative QCD [17], based essentially on the Coulombic interquark potential $V(R) = -4/3 \times \alpha_s(R)/R$. The cross section is built up by the superposition of all $nS(t\bar{t})$ states. The form and the height of the excitation curve are very sensitive to the mass of the top quark, Fig. 1.

Detailed experimental simulations predict the following sensitivity to the top mass [19] near $m_t \sim 175$ GeV:

$$\delta m_t \quad \lesssim \quad 200 \text{ MeV}$$

for an integrated luminosity of $\int \mathcal{L} = 50$ fb^{-1}, remnant uncertainties due to higher–order QCD corrections and experimental errors contributing at approximate equal strength. At proton colliders a sensitivity of about 2 GeV has been claimed for the top mass, based on the reconstruction of top quarks from jet and lepton final states. Thus, e^+e^- colliders will improve the measurement of the top quark mass by at least an order of magnitude.

3 Electroweak Gauge Bosons

3.1 Standard W, Z Bosons

The fundamental electroweak and strong forces appear to be of gauge theoretical origin. This is one of the outstanding results of theoretical and experimental analyses in the past three decades. However, little

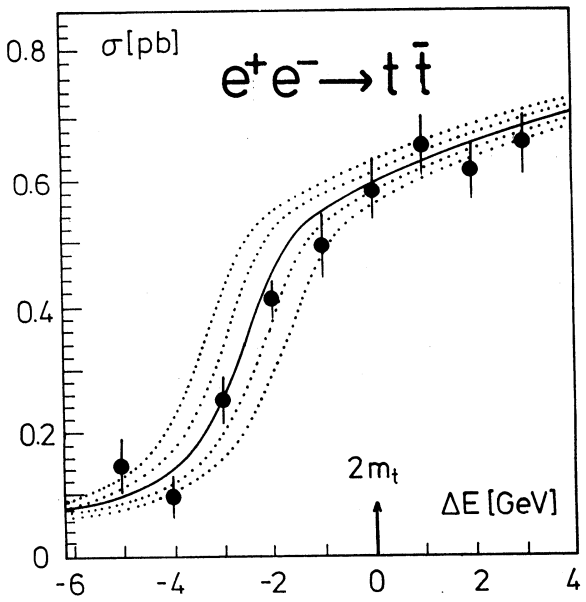

Figure 1: *The excitation curve for top production near the threshold; Ref.[18].*

direct evidence has been accumulated so far for the non–abelian nature of the forces in the electroweak $W^{\pm}, Z, \gamma$ sector. Since deviations from the gauge symmetries manifest themselves in experimental observables with coefficients $(\beta\gamma)^2$, high energies will allow stringent direct tests of the self–couplings of the electroweak gauge bosons.

The gauge symmetries of the Standard Model determine the form and the strength of the self–interactions of the electroweak bosons, triple couplings $WW\gamma, WWZ$ and quartic couplings. Deviations from the gauge symmetry form of these vertices could be expected in more general scenarios [20]. In models in which W, Z bosons are generated dynamically and interact strongly with each other at high scales Λ, corrections could alter the vertices to order $(M_W/\Lambda)^2$ and induce new types of couplings.

While the experimental analyses of the self–couplings of the electroweak bosons can be carried out at collider energies of 500 GeV with high accuracy, WW scattering [21] can only be studied at energies in the TeV range. This is an important process which must be investigated very thoroughly if light Higgs particles do not exist and W bosons become strongly interacting particles at high energies.

The properties of the Z boson have been studied at LEP and SLC with very high accuracy. By operating TESLA at low energies on the Z resonance in the GigaZ mode and near the WW threshold, the measurement of fundamental electroweak parameters, mixing angle and W mass can be improved by yet an order of magnitude, allowing to test electroweak symmetry breaking stringently at the quantum level.

The GigaZ Mode: By building a bypass for the transport of electron and positron bunches, high luminosity can also be reached at low energies. On the Z resonance, an ensemble of 10^9 events, 1 GigaZ, can be generated in a year, expanding the LEP sample by two orders of magnitude. With both electron and positron beams longitudinal polarized, the electroweak mixing angle can be determined very accurately by measuring the left–right asymmetry [22]

$$A_{LR} = \frac{2\,(1 - 4\sin^2\theta_W)}{1 + (1 - 4\sin^2\theta_W)^2} \quad : \quad \delta \sin^2\theta_W \approx 10^{-5}$$

Similarly the measurement of the W mass can be improved to

$$\delta M_W \approx 6\,\mathrm{MeV}$$

by scanning the threshold region [23].

Based on these two measurements, many high–precision tests can be performed in the electroweak sector. Extracting the Higgs mass from the electroweak observables is particularly interesting. From the ρ–parameter [26] this mass can be predicted to an accuracy of about 6%, improving LHC based predictions by almost an order of magnitude [24]. Comparing this prediction with the direct measurement of the Higgs mass, quantum fluctuations can be tested stringently in a spontaneously broken gauge theory.

The Triple Gauge Boson Couplings: The couplings $W^+W^-\gamma$ and W^+W^-Z are in general described each by seven parameters. Assuming $\mathcal{C}, \mathcal{P}$ and $\mathcal{T}$ invariance in the pure electroweak boson sector, the number of parameters can be reduced to three,

$$\mathcal{L}_j/g_j \;=\; ig_j^1 W^*_{\mu\nu} W_\mu A_\nu + \text{h.c.} \;+\; i\kappa_j W^*_\mu W_\nu F_{\mu\nu} \;+\; i\frac{\lambda_j}{M_W^2} W^*_{\rho\mu} W_{\mu\nu} F_{\nu\rho}$$

with $g_\gamma = e$ and $g_Z = e\cot\theta_W$ for $j = \gamma, Z$. The $\kappa = 1 + \Delta\kappa$ and the λ parameters can be identified with the γ, Z charges of the W bosons and the related magnetic dipole moments and electric quadrupole moments,

$$\begin{aligned} \mu_\gamma &= \tfrac{e}{2M_W}\Big[2 + \Delta\kappa_\gamma + \lambda_\gamma\Big] \quad \text{and} \quad \gamma \to Z \\ Q_\gamma &= -\tfrac{e}{M_W^2}\Big[1 + \Delta\kappa_\gamma - \lambda_\gamma\Big] \quad \text{and} \quad \gamma \to Z \end{aligned}$$

The gauge symmetries of the SM demand $\kappa = 1$ and $\lambda = 0$. The magnetic dipole and the electric quadrupole moments can be measured *directly* through the production of $W\gamma$ and WZ pairs at $p\overline{p}/pp$ colliders and WW pairs at e^+e^- and $\gamma\gamma$ colliders.

Detailed experimental analyses have been carried out for the reaction $e^+e^- \to W^+W^- \to (l\nu_e)(q\overline{q}')$. The bounds on $\Delta\kappa, \lambda$ which can be obtained at e^+e^- colliders of 500 GeV [25] are significantly better than the bounds expected from the LHC:

$$\begin{aligned} \delta\kappa_\gamma &= 4.8 \times 10^{-4} \qquad & \delta\kappa_Z &= 7.9 \times 10^{-4} \\ \lambda_\gamma &= 7.2 \times 10^{-4} \qquad & \delta\lambda_Z &= 6.5 \times 10^{-4} \\ & & \delta g_1^Z &= 2.5 \times 10^{-3} \end{aligned}$$

Moreover, they improve at 1 TeV by nearly an order of magnitude. The scales Λ which can be probed, extend far beyond the energy scales which are accessible directly.

Strongly Interacting W, Z Bosons If the scenario in which W, Z, Higgs bosons are weakly interacting up to the GUT scale is not realized in Nature, the alternative scenario is a strongly interacting W, Z sector. Without a light Higgs boson with a mass of less than about 1 TeV, the electroweak bosons must become strongly interacting particles at energies of about 1.2 TeV to comply with the requirements of unitarity for the W_LW_L scattering amplitudes. Based on Goldstone particles associated with the spontaneous symmetry breaking, the new strong interactions may build up the longitudinal degrees of freedom for the massive vector bosons in technicolor type theories, for instance. In such scenarios, novel resonances could be realized in the $\mathcal{O}(1\,\text{TeV})$ energy range, generated in W_LW_L collisions.

In scenarios of strongly interacting vector bosons, W_LW_L scattering must be studied at energies of order 1 TeV which requires the highest energies possible in e^+e^- colliders. (Quasi)elastic WW scattering can be investigated by using W bosons radiated off the electron and positron beams, $ee \to \nu\nu WW$, or by exploiting final state interactions in the e^+e^- annihilation to W pairs, $e^+e^- \to W^+W^-$. All possible (isospin, angular momentum) combinations in WW scattering amplitudes a_{IJ} can be realized in the first process. The cross sections however are small as long as no resonances are formed.

Building up the electroweak vector boson masses by the interactions of the gauge fields with the Goldstone bosons associated with the spontaneous symmetry breaking of the underlying strong–interaction theory, the longitudinal degrees of freedom of the vector bosons can be identified at high energies with the Goldstone bosons themselves as a result of the equivalence theorem. In analogy to the $\pi\pi$ low–energy theorems, the first terms in the energy expansion of the WW scattering amplitudes [27] are determined

independent of dynamical details:

$$a_{00} = +\frac{6}{96\pi v^2} \qquad a_{20} = -\frac{2}{96\pi v^2}$$

$$a_{11} = +\frac{1}{96\pi v^2}$$

These fundamental scattering amplitudes in the threshold region of the strong WW interactions can be tested to an accuracy of about 15% at a high–luminosity collider of 1 TeV [28].

The attractive $I = 0$ and $I = 1$ channels may form Higgs and ρ–type resonances at high energies. The formation of resonances would lead to spectacular phenomena in WW collisions [29].
Similar phenomena would also be observed as rescattering effects in the cross section $\sigma(e^+e^- \to W^+W^-)$ for W–pair production. $(I, J) = (1, 1)$ resonance effects would be noticeable at $\sqrt{s} = 1$ TeV up to resonance masses of about 5 TeV in the angular distributions of the W decay final states [30].

3.2 Extended Gauge Theories

The gauge symmetry of the Standard Model, $\mathrm{SU}(3) \times \mathrm{SU}(2) \times U(1)$, is widely believed not to be the *ultima ratio*. The SM does not unify the electroweak and strong forces since the coupling constants of these interactions are different and appear to be independent. However, one should expect that in a more fundamental theory the three forces are described within a single gauge group and, hence, with only one coupling constant at high energy scales. This grand unified theory will be based on a gauge group containing $SU(3) \times SU(2) \times U(1)$ as a subgroup and it will be reduced to this symmetry at low energies.

Two predictions of grand unified theories may have interesting consequences in the energy range of a few hundred GeV [31]:

(i) The unified symmetry group must be spontaneously broken at the unification scale $\Lambda_{\mathrm{GUT}} \gtrsim 10^{16}$ GeV in order to be compatible with the experimental bounds on the proton lifetime. However, the breaking to the SM group may occur in several steps and some subgroups may remain unbroken down to a scale of order 1 TeV. In this case the surviving group factors allow for new gauge bosons with masses not far above the scale of electroweak symmetry breaking. Besides SU(5), two other unification groups have received much attention: In SO(10) three new gauge bosons $W_R^{\pm}, Z_R$ are predicted, while in E(6) a light neutral Z' boson may exist in the TeV range.

The virtual effects of a new Z_R, Z' boson associated with the most general effective theories which arise from breaking $\mathrm{E}(6) \to \mathrm{SU}(3) \times \mathrm{SU}(2) \times \mathrm{U}(1) \times \mathrm{U}(1)_{\mathrm{Y}'}$ and $\mathrm{SO}(10) \to \mathrm{SU}(2)_{\mathrm{L}} \times \mathrm{SU}(2)_{\mathrm{R}} \times \mathrm{U}(1)$, have been investigated in Ref. [32]. Assuming the Z_R, Z' bosons to be heavier than the available c.m. energy, the propagator effects on various observables of the process

$$e^+e^- \xrightarrow{V} f\bar{f} : \quad V = \gamma, Z \text{ and } Z_R, Z'$$

have been studied in detail. As shown in Table 1, the effects of new vector bosons can be probed for masses up to 5 TeV at a 500 GeV collider. While they may be produced directly up to about 5 TeV at the LHC, experiments at the e^+e^- collider will measure the couplings of the vector bosons to fermions very precisely, thus identifying the physical nature of the new bosons. Masses up to 10 TeV and 50 TeV can be probed in e^+e^- colliders operating at 800 GeV and 5 TeV, respectively. These two windows extend to much higher scales than the discovery limits anticipated at LHC.

(ii) The grand unification groups incorporate extended fermion representations in which a complete generation of SM quarks and leptons can be naturally embedded. These representations accommodate a variety of additional new fermions. It is conceivable that the new fermions acquire masses not much larger than the Fermi scale. This is necessary if the predicted new gauge bosons are relatively light. SO(10) is the simplest group in which the 15 members of each SM generation of fermions can be embedded into a single multiplet. This representation has dimension **16** and contains a right–handed neutrino. The group E(6) contains SU(5) and SO(10) as subgroups. In E(6), each quark–lepton generation belongs to a representation of dimension **27**. To complete this representation, twelve new fields are needed in addition to the SM fermion fields. In each family the spectrum includes two additional isodoublets of leptons, two isosinglet neutrinos and an isosinglet quark with charge $-1/3$.

$\sqrt{s}$	SO(10)	E(6)
500 GeV	6 TeV	5–7 TeV
800 GeV	10 TeV	8–11 TeV
5 TeV	$\sim$ 50 TeV	$\sim$ 50 TeV

Table 1: *Sensitivity limits of Z_R masses in SO(10) and Z' masses in E(6) at e^+e^- linear colliders in the TeV range.*

If the new particles have non–zero electromagnetic and weak charges, and if their masses are smaller than the beam energy of the e^+e^- collider, they can be pair produced. In general, the production processes are built up by a superposition of s–channel γ and Z exchanges, but additional contributions could come from the extra neutral bosons if their masses are not much larger than the c.m. energy [31]. The cross sections are large, of the order of the point–like QED cross section. This leads to samples of several thousands of events. Fermion mixing, if large enough, gives rise to additional production mechanisms for the new fermions: single production in association with the light partners. In this case, masses very close to the total energy of the e^+e^- collider can be reached.

4 Higgs Bosons

The Higgs mechanism is the cornerstone in the electroweak sector of the Standard Model. The fundamental SM particles, leptons, quarks and weak gauge bosons, acquire masses through the interaction with a scalar field. To accommodate the well–established electromagnetic and weak phenomena, the Higgs mechanism requires the existence of at least one weak iso–doublet scalar field. After absorbing three Goldstone modes to build up the longitudinal polarization states of the $W^\pm, Z$ bosons, one degree of freedom is left–over, corresponding to a real scalar particle.

Three steps are necessary to establish the Higgs mechanism *sui generis* experimentally as the mechanism for generating the masses of the fundamental SM particles:

(i) The Higgs boson must be discovered, the *experimentum crucis*.

(ii) It must be proven that the couplings of the Higgs particle with gauge bosons and fermions increase with their masses;

(iii) The Higgs potential generating the non–zero Higgs field in the vacuum and breaking the electroweak symmetry in the scalar sector must be reconstructed by determining the Higgs self–couplings.

The only unknown parameter in the SM Higgs sector is the mass of the Higgs particle. Constraints on the mass can, however, be derived from the upper scale Λ of the energy range in which the model is assumed to be valid before the particles become strongly interacting and new dynamical phenomena emerge [33]. Increasing the energy scale, the quartic self–coupling of the Higgs field grows logarithmically for large values indefinitely. If the Higgs mass is small, the energy cut–off Λ is large at which the coupling grows beyond any bound; conversely, if the Higgs mass is large, the cut–off Λ is small. The condition $M_H < \Lambda$ sets an upper limit on the Higgs mass in the Standard Model. Detailed analyses lead to an estimate of about 700 GeV for the upper limit on M_H. If the Higgs mass is less than 180 to 200 GeV, the Standard Model can be extended up to the GUT scale $\Lambda_{\rm GUT} \sim 10^{16}$ GeV, while all particles remain weakly interacting. The hypothesis that interactions between W, Z bosons and Higgs particles remain weak up to the GUT scale, plays a key rôle in deriving the experimental value of the electroweak mixing parameter $\sin^2\theta_W$ from grand unified theories. From this hypothesis and the additional requirement of vacuum stability, upper and lower bounds on the Higgs mass can be derived. Based on these arguments, the SM Higgs mass should be expected in the mass window $130 < M_H < 180$ GeV for a top mass value of about 175 GeV.

A large variety of channels can be exploited to search for Higgs particles in the Higgs–strahlung and fusion processes of e^+e^- colliders [34, 35, 36]. In the Higgs–strahlung process $e^+e^- \to ZH$, missing–mass techniques can be used in events with leptonic Z decays or the Higgs particle may be reconstructed in $H \to b\bar{b}, WW$ directly. The WW fusion process $e^+e^- \to \bar{\nu}_e\nu_e H$ requires the reconstruction of the Higgs particle.

Once the Higgs boson is found at LEP, Tevatron or LHC, it will be very important to explore its properties at the e^+e^- linear collider to establish the Higgs mechanism *sui generis* experimentally. This is possible with high precision in the clean environment of e^+e^- colliders in which at high luminosity a large ensemble of order 10^5 Higgs bosons can be generated nearly background–free. The zero–spin of the Higgs particle is reflected in the angular distribution of the Higgs–strahlung process which asymptotically must approach the $\sin^2\theta$ law. The strength of the couplings to Z and W bosons is reflected in the magnitude of the e^+e^- production cross sections. The strength of the couplings to fermions can be measured through the decay branching ratios and Higgs bremsstrahlung off top quarks. Double Higgs–strahlung can be exploited to measure the trilinear Higgs self–coupling.

From the preceding discussion we conclude that an e^+e^- linear collider with energies in the range of 300 to 500 GeV and high luminosity is the ideal instrument to investigate the Higgs mechanism in the intermediate mass range which, *a priori*, may be considered the most important part in the entire range of possible Higgs mass values. A similarly comprehensive analysis can be performed in supersymmetric extensions of the Standard Model. In particular, the Minimal Supersymmetric extension of the Standard Model MSSM incorporates a spectrum of five Higgs particles (representative for a wide class of models), which can be explored in all facets at e^+e^- colliders. At tree level, the mass of the lightest Higgs boson h^0 is smaller than the Z mass; the bound is shifted to ~ 150 GeV by radiative corrections. This particle is guaranteed to be detected at e^+e^- colliders — even in non–minimal versions of the supersymmetric theories. The masses of the heavy neutral and charged Higgs bosons can be expected in the range of the electroweak symmetry breaking scale so that a large part of the mass parameter space can be covered for the individual Higgs particles at e^+e^- colliders operating at an energy of 1 TeV. The detailed comparison of branching ratios and production cross sections with the predictions of the MSSM will eventually shed light on the physical basis of the extended Higgs sector.

4.1 The Higgs Particle in the Standard Model

The profile of the SM Higgs particle is completely determined if the Higgs mass is fixed. For Higgs particles in the intermediate mass range $M_Z \leq M_H \leq 2M_Z$ the main decay modes are decays into $b\bar{b}$ pairs and WW, ZZ pairs with one of the two gauge bosons being virtual below the threshold [37]. Above the WW threshold, the Higgs particles decay almost exclusively into these channels, except in the mass range near the $t\bar{t}$ decay threshold. Below 140 GeV, the decays $H \to \tau^+\tau^-, c\bar{c}$ and gg are also important besides the dominating $b\bar{b}$ channel. Up to masses of 140 GeV, the Higgs particle is very narrow, $\Gamma(H) \leq 10$ MeV. After opening the [virtual] gauge boson channels, the state becomes rapidly wider, reaching ~ 1 GeV at the ZZ threshold. The width cannot be measured directly in the intermediate mass range. Only above $M_H \geq 200$ GeV it becomes wide enough to be resolved experimentally.

The main production mechanisms for Higgs particles in e^+e^- collisions are Higgs–strahlung off the Z boson line [38] and the WW fusion process [39],

$$\begin{aligned} e^+e^- &\xrightarrow{Z} Z + H \\ e^+e^- &\xrightarrow{WW} \bar{\nu}_e\ \nu_e\ + H \end{aligned}$$

With rising energy the Higgs–strahlung cross section scales $\sim \alpha_w^2/s$ while the fusion cross sections increase logarithmically $\sim \alpha_w^3 M_W^{-2} \log s/M_H^2$, becoming dominant above 500 GeV:

$$\begin{aligned} \sigma(e^+e^- \to ZH) &\to \frac{G_F^2 M_Z^4}{96\pi s}[1 + (1 - 4\sin^2\theta_W)^2] \\ \sigma(e^+e^- \to \bar{\nu}\nu H) &\to \frac{G_F^3 M_W^4}{4\sqrt{2}\pi^3} \log\frac{s}{M_H^2} \end{aligned}$$

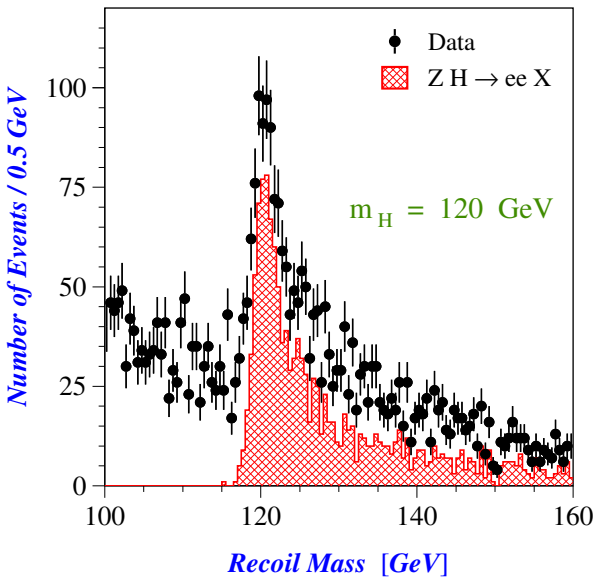

Figure 2: *Production of Higgs particles in the Higgs–strahlung channel* $e^+e^- \to ZH \to e^+e^-X$*; Ref.[40].*

As a general rule, the cross sections and rates [about 10^5 events] are sufficiently large to detect Higgs particles with masses up to 70% of the total e^+e^- c.m. energy.

The recoiling Z boson in the two–body reaction $e^+e^- \to ZH$ is mono–energetic and the mass can be derived from the energy of the Z boson, $M_H^2 = s - 2\sqrt{s}E_Z + M_Z^2$. Initial state bremsstrahlung and beamstrahlung smear out the peak slightly, as shown in Fig. 2. A similarly clear peak can be observed in the fusion process $e^+e^- \to \overline{\nu}_e\nu_e H$ by collecting the decay products of the Higgs boson.

Mass and Width: The mass of the Higgs boson can be measured very accurately by analyzing the recoil Z spectrum in Higgs–strahlung events. Experimental simulations [41] have demonstrated that the error in the mass measurement can be reduced to

$$\delta M_H \lesssim 50\,\mathrm{MeV}$$

in high–luminosity runs.

The width of the SM Higgs boson can be determined in an almost completely model–independent way in the difficult intermediate mass range in which the Breit–Wigner form cannot be reconstructed at an e^+e^- collider. Measuring the branching ratio BR_i in the decay and the partial width Γ_i in the production process, the total width Γ_H can be derived from

$$\Gamma_H = \Gamma_i / BR_i$$

The two channels $i = WW$ [42, 43] and $i = \gamma\gamma$ [44] are useful for this analysis [45]. The partial width Γ_{WW} can be extracted from the size of the WW fusion cross section [46] while $\Gamma_{\gamma\gamma}$ can be measured in the Compton collider mode [47]. The accuracies of a few percent match the expected accuracy in scanning the Breit–Wigner excitation in a muon–collider.

Spin and Parity: The angular distribution of the Z/H bosons in the Higgs–strahlung process is sensitive to the external quantum numbers of the Higgs particle [38]. Since the amplitude is given by $\mathcal{A}(0^+) \sim \varepsilon_1 \cdot \varepsilon_2$, the Z boson is produced in a state of longitudinal polarization at high energies. As a result, the angular distribution $\mathrm{d}\sigma/\mathrm{d}\cos\theta \sim \lambda \sin^2\theta + 8M_Z^2/s$ approaches the spin–zero law $\sin^2\theta$ asymptotically. This may be contrasted with the distribution $\sim 1 + \cos^2\theta$ for negative parity states, which follows from the transverse polarization amplitude $\mathcal{A}(0^-) \sim \varepsilon_1 \times \varepsilon_2 \cdot k_Z$. It is also characteristically different from the background process $e^+e^- \to ZZ$ which is strongly peaked in the forward/backward direction.

Higgs Couplings: Since the fundamental SM particles acquire masses through the interaction with the Higgs field, the scale of the Higgs couplings to fermions and gauge bosons is set by the masses of the particles:

$$g_{HVV} = 2[\sqrt{2}G_F]^{1/2} M_V^2 \qquad \text{and} \qquad g_{Hff} = [\sqrt{2}G_F]^{1/2} M_f$$

It will be a very important task to measure the Higgs couplings to the fundamental particles [42, 43] since they are uniquely predicted by the very nature of the Higgs mechanism. The Higgs couplings to massive gauge bosons can be determined from the measurement of the production cross sections with an accuracy of $\pm 1\%$, the HZZ coupling in the Higgs–strahlung and the HWW coupling in the fusion process. For Higgs couplings to fermions, either loop effects in $H \rightleftharpoons gg, \gamma\gamma$ [mediated by top quarks] can be exploited, or the direct measurement of branching ratios $H \to b\overline{b}, c\overline{c}, \tau^+\tau^-, gg$ in the lower part of the intermediate mass range. This is exemplified in Fig. 3. For $M_H = 120\,\text{GeV}$ the following accuracy $\delta BR/BR$ can be achieved [43] in the determination of the Higgs decay branching ratios:

$$\begin{aligned} bb &: 2.4\% & \qquad WW^* &: 5.4\% \\ cc &: 8.3\% & \qquad gg &: 5.5\% \\ \tau\tau &: 6.0\% & & \end{aligned}$$

By measuring the ratio of the $\tau\tau$ to the bb branching ratios

$$\frac{BR(H \to \tau\tau)}{BR(H \to bb)} = \frac{m_\tau^2}{3m_b^2(M_H)}$$

the linear dependence of the Yukawa couplings on the fermion masses can be tested very nicely. A direct way to determine the Yukawa coupling of the intermediate mass Higgs boson to the top quark in the range $m_H \leq 120\,\text{GeV}$ is provided by the bremsstrahlung process $e^+e^- \to t\bar{t}H$ in high energy e^+e^- colliders [48]. The absolute values of the Yukawa couplings can be reconstructed by combining decay branching ratios with the production cross sections.

Higgs Self–couplings: To generate a non–zero value of the Higgs field in the vacuum, the minimum of the Higgs potential must be shifted away from the origin. Rewriting the potential

$$\begin{aligned} V &= \lambda\,[|\,\varphi\,|^2 - \tfrac{1}{2}\,v^2]^2 \\ &= \frac{M_H^2}{2}\,H^2 + \frac{M_H^2}{2v}\,H^3 + \frac{M_H^2}{8v^2}\,H^4 \end{aligned}$$

in terms of the physical Higgs field H, the potential can be reconstructed by measuring the trilinear and quartic couplings. At a high–luminosity e^+e^- collider, the trilinear coupling can be tested in the double Higgs–strahlung process

$$e^+e^- \to Z + HH$$

The splitting of a virtual Higgs boson into two real Higgs bosons is determined by the trilinear Higgs coupling: $e^+e^- \to Z + H^*\,[\to HH]$. Even though the cross section is less than 1 fb [49], the coupling can be expected nevertheless to be measured with an accuracy better than 20% [50]. Thus an essential element of the mechanism responsible for the spontaneous symmetry breaking in the scalar sector can be established experimentally at the high–luminosity collider.

4.2 SUSY Higgs Particles

The Higgs spectrum in the minimal supersymmetric extension of the Standard Model [51] consists of five states: h^0, H^0, A^0 and $H^\pm$. Besides the masses, two mixing angles define the properties of the scalar particles and their interactions with gauge bosons, fermions and the self–interactions: the ratio of the two vacuum expectation values $\text{tg}\beta = v_2/v_1$ and a mixing angle α in the neutral CP–even sector. Supersymmetry leads to several relations among the masses and mixing angles, and, in fact, only two parameters are independent.

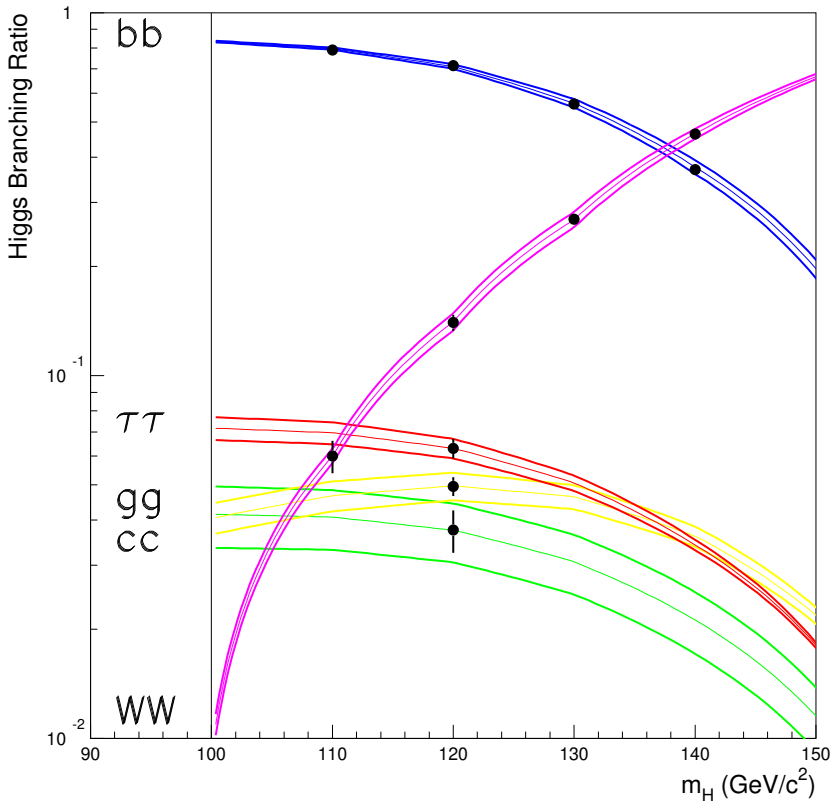

Figure 3: *Branching ratios of SM Higgs decays into fermion and WW^* pairs; Ref.[43].*

Neutral Higgs Bosons: The lightest neutral Higgs boson will decay mainly into fermion pairs since its mass is smaller than ~ 150 GeV. This is also the dominant decay mode of the pseudoscalar boson A^0. For values of tgβ larger than unity and for masses less than ~ 140 GeV, the main decay modes of the neutral Higgs bosons are decays into $b\bar{b}$ and $\tau^+\tau^-$ pairs; the branching ratios are of order $\sim 90\%$ and 8%, respectively. The decays into $c\bar{c}$ pairs and gluons [proceeding through t and b quark loops] are suppressed, for large tgβ strongly. For large masses, the top decay channels $H^0, A^0 \to t\bar{t}$ open up; yet this mode remains suppressed for large tgβ. For large tgβ, the neutral Higgs bosons decay almost universally into $b\overline{b}$ and $\tau^+\tau^-$ pairs. If the mass is high enough, the heavy CP–even Higgs boson H^0 can in principle decay into weak gauge bosons, $H^0 \to WW, ZZ$. Since the partial widths are proportional to $\cos^2(\beta-\alpha)$, they are strongly suppressed and the gold–plated ZZ signal of the heavy SM Higgs boson is lost in the supersymmetric extension. The heavy neutral Higgs boson H^0 can also decay into two lighter Higgs bosons. These modes, however, are restricted to small domains in the parameter space. Other possible channels are decays into supersymmetric particles. While sfermions are likely too heavy to affect Higgs decays in the mass range considered here, Higgs boson decays into charginos and neutralinos could eventually be important since the masses of some of these particles are expected to be of order M_Z. [These new channels are summarized in Ref.[52].] The charged Higgs particles decay into fermions but also, if allowed kinematically, into the lightest neutral Higgs boson and a W boson. Below the tb and Wh thresholds, the charged Higgs particles will decay mostly into $\tau\overline{\nu}_\tau$ and $c\bar{s}$ pairs, the former being dominant for tg$\beta > 1$. For large $M_{H^\pm}$ values, the top–bottom decay mode $H^+ \to t\bar{b}$ becomes dominant.

Adding up the various decay modes, the width of all five Higgs bosons remains very narrow, being of order 10 GeV even for large masses.

The search for the neutral SUSY Higgs bosons at e^+e^- colliders will be a straightforward extension of the search performed at LEP2. This collider is expected to cover the mass range up to ~ 90 to 100 GeV for neutral Higgs bosons, depending on tgβ. Higher energies, $\sqrt{s} \sim 250$ GeV, are required to sweep the entire parameter space of the MSSM . The main production mechanisms of neutral Higgs bosons at e^+e^- colliders [52, 51] are the Higgs–strahlung process and associated pair production,

$$\begin{array}{lll} (a) \quad \text{Higgs} - \text{strahlung} & e^+e^- & \to \quad Z + h/H \\ (b) \quad \text{pair production} & e^+e^- & \to \quad A + h/H \end{array}$$

as well as the related fusion processes. The CP–odd Higgs boson A^0 cannot be produced in fusion processes since it does not couple to gauge bosons in leading order.

The cross sections for the four Higgs–strahlung and pair production processes can be expressed as

$$\begin{aligned} \sigma(e^+e^- \to Zh) &= \sin^2(\beta-\alpha)\ \sigma_{SM} \\ \sigma(e^+e^- \to ZH) &= \cos^2(\beta-\alpha)\ \sigma_{SM} \end{aligned}$$

and

$$\begin{aligned} \sigma(e^+e^- \to Ah) &= \cos^2(\beta-\alpha)\ \bar{\lambda}\ \sigma_{SM} \\ \sigma(e^+e^- \to AH) &= \sin^2(\beta-\alpha)\ \bar{\lambda}\ \sigma_{SM} \end{aligned}$$

where σ_{SM} is the SM cross section for Higgs–strahlung and the factor $\bar{\lambda}$ accounts for the suppression of the P–wave cross sections near the threshold. The cross sections for the Higgs–strahlung and for the pair production as well as the cross sections for the production of the light and the heavy neutral Higgs bosons h^0 and H^0 are mutually complementary to each other, coming either with a coefficient $\sin^2(\beta-\alpha)$ or $\cos^2(\beta-\alpha)$. As a result, since σ_{SM} is large, at least the lightest CP–even Higgs boson must be detected.

The cross section for hZ in the Higgs–strahlung process is large for values of M_h near the upper bound. The heavy CP–even and CP–odd Higgs bosons H and A, on the other hand, are produced pairwise in this limit:

$$e^+e^- \to HA$$

The decoupling limit corresponds to heavy Higgs masses above 250 to 300 GeV. The discovery limit is therefore set by the beam energy independently of the mixing parameter tgβ, in contrast to LHC where the heavy Higgs bosons cannot be detected individually in parts of the parameter space.

Charged Higgs Bosons: The charged Higgs bosons, if lighter than the top quark, can be produced in top decays, $t \to b + H^+$, with a branching ratio varying between 2% and 20% in the kinematically allowed region. Since for tgβ larger than unity, the charged Higgs bosons will decay mainly into $\tau\nu_\tau$, this results in a surplus of τ final states over e, μ final states in t decays, an apparent breaking of lepton universality. For large Higgs masses the dominant decay mode is the top decay $H^+ \to t\bar{b}$. In this case the charged Higgs particles must be pair produced in e^+e^- colliders:

$$e^+e^- \to H^+H^-$$

The cross section depends only on the charged Higgs mass. For small Higgs masses the cross section is of order 100 fb at $\sqrt{s} = 500$ GeV, but it drops very quickly due to the P–wave suppression $\sim \beta^3$ near the threshold.

The preceding discussion of the MSSM Higgs sector at e^+e^- linear colliders can be summarized in the following two points:
(i) The lightest CP–even Higgs particle h^0 can be detected in the entire range of the MSSM parameter space, either through the Higgs–strahlung process $e^+e^- \to hZ$ or through pair production $e^+e^- \to hA$ [41]. In fact, this conclusion holds true even at a c.m. energy of 250 GeV, independent of the top and squark mass values, and also if invisible neutralino decays are allowed for.
(ii) The area in the parameter space where *all* SUSY Higgs bosons individually can be discovered at e^+e^- colliders is characterized by $M_A \lesssim \frac{1}{2}\sqrt{s}$, independently of tg$\beta$. The H^0, A^0 Higgs bosons can be produced either through Higgs–strahlung or through Ah, AH associated production; charged Higgs bosons will be produced in H^+H^- pairs up to the kinematical limit.

5 Supersymmetry

Even though there is no direct experimental evidence so far for the realization of supersymmetry in Nature, this concept has so many attractive features that it can be considered as a prime target of present and future experimental particle research [53]. Arguments in favor of supersymmetry are deeply rooted in particle physics. Supersymmetry may play an important rôle in a quantum theory of gravity. In relating particles of different spins to each other, i.e. fermions and bosons, low–energy supersymmetry stabilizes the masses of fundamental Higgs scalars in the background of very high energy scales associated with grand unification. Besides solving this hierarchy problem, supersymmetry may even be closely related to the physical origin of the Higgs phenomenon itself: In a supergravity inspired GUT realization with universal scalar masses at the GUT scale, the evolution of one of the scalar masses squared can become negative and can thus give rise to spontaneous symmetry breaking if the top mass has a value between about 100 to 200 GeV while all other squared masses of squarks and sleptons remain positive so that $U(1)_{EM}$ and $SU(3)_C$ remain unbroken.

The minimal supersymmetric extension of the Standard Model is based on the SM group $SU(3) \times SU(2) \times U(1)$. The gauginos are the supersymmetric spin–$\frac{1}{2}$ partners of the gauge bosons. The quark and lepton matter particles are associated with scalar supersymmetric particles, squarks and sleptons. To preserve supersymmetry, two Higgs doublets are needed to endow down as well as up–type fermions with masses; the supersymmetric partners of the Higgs bosons are spin–$\frac{1}{2}$ higgsinos. [Charged/neutral higgsinos mix in general with the non–colored gauginos, forming charginos and neutralinos.] Supersymmetric partners carry a multiplicative quantum number $R = -1$ ($R = +1$ for ordinary particles) which is conserved in this model. Supersymmetric particles are therefore generated in pairs and the lightest supersymmetric particle LSP is stable.

Strong support for supersymmetry and the MSSM particle spectrum in the mass range of several hundred GeV follows from the high–precision measurement of the electroweak mixing angle $\sin^2\theta_W$ [58]. The value predicted by the MSSM and the value determined by the LEP and other experiments,

$$\begin{aligned} MSSM: \quad & \sin^2\theta_W = 0.2336 \pm 0.0017 \\ EXP \quad : \quad & \sin^2\theta_W = 0.2316 \pm 0.0002 \end{aligned}$$

match surprisingly well, the difference being less than about 2 per–mille.

A central problem of supersymmetric theories is the breaking mechanism. Several scenarios have been proposed and experimental consequences have been elaborated in a few cases: gravity mediated supersymmetry breaking mSUGRA [54]; gauge mediated supersymmetry breaking GMSB [55]; anomaly mediated supersymetry breaking AMSB [56]; Scherk–Schwarz supersymmetry breaking SSSB [57]. Mass spectra of the supersymmetric particles are quite different in these scenarios so that high–precision measurements of the particle properties will shed light experimentally on this theoretical problem. Moreover, extrapolations can be performed in a stable way which will allow to reconstruct the basic supersymmetric theory eventually at a scale close to the Planck scale. High–precision experiments at a high–luminosity e^+e^- linear collider are expected to advance the understanding of supersymmetry in an essential way.

5.1 Supersymmetric Particles

Charginos and Neutralinos The two charginos $\tilde{\chi}_i^+$ and the four neutralinos $\tilde{\chi}_i^0$, mixtures of the [non–colored] gauginos and higgsinos, are expected to be the lightest supersymmetric particles. In the MSSM with conserved R–parity, the neutralino $\tilde{\chi}_1^0$ with the smallest mass, assumed to be the lightest supersymmetric particle, is stable. The heavier neutralinos and the charginos decay into (possibly virtual) gauge and Higgs bosons plus the LSP, $\tilde{\chi}_i^0 \longrightarrow \tilde{\chi}_1^0 + Z$ and $\tilde{\chi}_1^0 + W$, or if they are heavy enough, into neutralino/chargino cascades, and leptons plus sleptons [59].

Neutralinos and charginos are easy to detect at e^+e^- colliders. They are produced in pairs

$$\begin{aligned} e^+e^- \quad &\longrightarrow \quad \tilde{\chi}_i^+ + \tilde{\chi}_j^- \qquad [i,j = 1,2] \\ e^+e^- \quad &\longrightarrow \quad \tilde{\chi}_i^0 + \tilde{\chi}_j^0 \qquad [i,j = 1,..,4] \end{aligned}$$

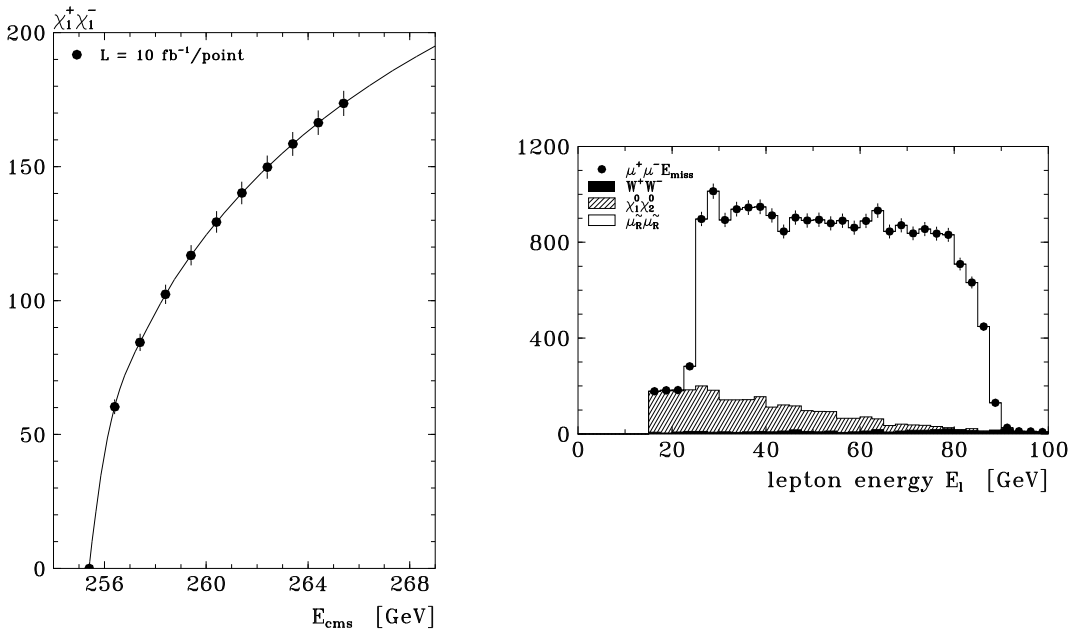

Figure 4: *The excitation curve for chargino production $e^+e^- \to \tilde{\chi}_1^+\tilde{\chi}_1^-$ near the threshold and energy distribution of the final state μ in the decay $\tilde{\mu}_R \to \mu + \tilde{\chi}_1^0$ in flight; Ref.[60].*

through s–channel γ, Z exchange and t–channel selectron or sneutrino exchange. Since the cross sections are as large as $\mathcal{O}(100$ fb), enough events will be produced to discover these particles for masses nearly up to the kinematical limit.

The properties of the charginos and neutralinos can be studied in great detail at e^+e^- colliders. From the fast onset $\sim \beta$ of the spin $-\frac{1}{2}$ excitation curve near the threshold, the masses can be measured very accurately within less than a hundred MeV. The decay spectra of heavier supersymmetric particles allow us to measure the mass of the LSP within $\pm\,2$ GeV, Fig. 4. Using polarized $e^\pm$ beams, the decomposition of the states, $\tilde{\chi}_i^+ = \alpha\tilde{W}^+ + \beta\tilde{H}^+$ into wino and higgsino components can be determined [61] since left–handed electrons couple to sneutrinos in the t–channel but right–handed electrons do not, so that the energy and angular dependence of the cross sections is different for the two polarization states [62]. In a similar way the properties of neutralinos can be explored [63].

Sleptons and Squarks: The superpartners of the right–handed leptons decay into the associated SM partners and neutralinos/charginos. In major parts of the SUSY parameter space the dominant decay mode is $\tilde{\mu}_R \to \mu + \tilde{\chi}_1^0$ [59]. For the superpartners of the left–handed sleptons, the decay pattern is slightly more complicated since, besides the $\tilde{\chi}_1^0$ channels, decays into leptons and charginos are also possible. In e^+e^- and e^-e^- collisions, sleptons are produced in pairs:

$$\begin{aligned}
e^+e^- &\longrightarrow \tilde{\mu}_L^+\tilde{\mu}_L^-\ ,\ \tilde{\mu}_R^+\tilde{\mu}_R^-\ ,\ \tilde{\tau}_L^+\tilde{\tau}_L^-\ ,\ \tilde{\tau}_R^+\tilde{\tau}_R^- \\
e^+e^- &\longrightarrow \tilde{\nu}_L\overline{\tilde{\nu}}_L \\
e^+e^- &\longrightarrow \tilde{e}_L^+\tilde{e}_L^-\ ,\ \tilde{e}_R^+\tilde{e}_R^-\ ,\ \tilde{e}_L^+\tilde{e}_R^-\ ,\ \tilde{e}_R^+\tilde{e}_L^- \\
e^-e^- &\longrightarrow \tilde{e}_L^-\tilde{e}_L^-\ ,\ \tilde{e}_R^-\tilde{e}_R^-\ ,\ \tilde{e}_L^-\tilde{e}_R^-
\end{aligned}$$

For charged sleptons, the production proceeds via γ, Z exchange in the s–channel, in the case of selectrons, also by additional t–channel neutralino exchange. For sneutrinos, the process is mediated by s–channel Z–exchange and, in the case of electron–sneutrinos, also by the t–channel exchange of charginos.

The cross sections for the pair production of sleptons are of the order of 10^{-1} to 10^{-2} pb so that their discovery is very easy up to the kinematical limit. From the P–wave onset $\sim \beta^3$ of the annihilation cross section the masses can in general be determined [60] at a level of 200 to 300 MeV; the sharper onset of selection production in e^-e^- scattering [64] will reduce this number further. Enough events will be produced to study their detailed properties. The polarization of the $e^\pm$ beams will help to identify the couplings of these particles.

If one of the stop states is light enough due to the strong LR Yukawa mixing, these particles may be pair produced even at a 500 GeV collider:

$$e^+e^- \to \tilde{t}_i + \overline{\tilde{t}_j} \qquad i,j = 1,2$$

By measuring the LR asymmetry of the production cross sections, the $\tilde{t}_L/\tilde{t}_R$ mixing angle can be determined to high accuracy $\delta \cos\theta_{\tilde{t}} \approx 0.01$ [65].

5.2 Testing SUSY –GUT

The high precision with which masses, couplings and mixing parameters will be determined at e^+e^- colliders, can be exploited to test the mechanism for supersymmetry breaking and the structure of underlying theories. In minimal supergravity mSUGRA the breaking of supersymmetry is mediated by gravity from a hidden sector to the eigenworld, generating soft SUSY breaking parameters at the grand unification scale [1]. The parameters are generally assumed to be universal at that scale in the gaugino and the scalar sectors. In gauge mediated supersymmetry breaking, gauge interactions connect the mechanism to the eigenworld at a scale possibly between 10 and 10^5 TeV. Mass spectra in mSUGRA and GMSB are characteristically different, the splitting between sleptons and squarks being larger in GMSB. Moreover, since the gravitino in GMSB is very light, $\tilde{\chi}_1^0$ or $\tilde{\tau}_1$ may be long lived giving rise to displaced photons or stable heavy tracks in the decays $\tilde{\chi}_1^0 \to \gamma\tilde{G}$ or $\tilde{\tau}_1 \to \tau\tilde{G}$ with the gravitino $\tilde{G}$ escaping undetected [66].

If minimal supergravity is the underlying theory, the observable properties of the superparticles can be expressed by a small set of parameters defined at the GUT scale. Basically four parameters specify the properties of the particles in the supersymmetric sector. The scalar mass parameter m_0, the $SU(2)$ gaugino mass $M_{1/2}$, the trilinear coupling A_0 and the sign of the coupling μ of the Higgs doublets in the superpotential, and $\tan\beta$, the ratio of the vacuum expectation values v_2/v_1. The Higgs sector requires another parameter which is in general identified with the mass of the pseudoscalar Higgs boson M_A. Evolving the scalar masses from the GUT scale down to low energies, it turns out that non–colored particles are in general significantly lighter than colored particles. The lightest of the non–colored gauginos/higgsinos and sleptons could have masses in the range of 100 to 200 GeV. Since only a few parameters determine the low energy theory of the evolution from the GUT scale down to the electroweak scale, many relations can be found among the masses of the superparticles which can stringently be tested at e^+e^- colliders. Two examples should illustrate the physics potential of the e^+e^- facilities in this context.

(i) The *gaugino masses* at the scale of $SU_2 \times U_1$ symmetry breaking are related to the common SU_2 gaugino mass $M_{1/2}$ at the GUT scale by the running gauge couplings:

$$M_i = \frac{\alpha_i}{\alpha_{GUT}} M_{1/2} \qquad i = SU_3, SU_2, U_1$$

with α_{GUT} being the gauge coupling at the unification scale. The mass relation in the non–color sector

$$\frac{M_1}{M_2} = \frac{5}{3}\tan^2\theta_W \approx \frac{1}{2}$$

[1] If gravitational interactions would become strong not at very high scale but near the electroweak scale [67], collider experiments could probe the additional spatial dimensions through which gravitational fields could propagate [68]. Contact interactions and missing energy events could signal Planck scales in 4 + n dimensions up to about 10 TeV. Thus, the basic space–time structure can be explored in these experiments.

Parameter	Theor. Value	Meas. Error
m_0	100 GeV	0.09 GeV
$M_{1/2}$	200 GeV	0.10 GeV
A_0	0 GeV	6.30 GeV
$\tan\beta$	3	0.02

Table 2: *Measurement of universal mSUGRA parameters.*

can be tested very well by measuring the masses and production cross sections of charginos/neutralinos and sleptons.

(*ii*) In a similar way the *slepton masses* can be expressed in terms of a common scalar mass parameter m_0 at the GUT scale, contributions $\sim M_{1/2}$ due to the evolution from the GUT scale down to low energies, and the D terms related to the electroweak symmetry breaking. These expressions give rise to relations among the slepton masses:

$$\begin{aligned} m^2(\tilde{l}_L) - m^2(\tilde{\nu}) &= -(1 - 2\sin^2\theta_W)\cos 2\beta m_Z^2 \\ m^2(\tilde{l}_L) - m^2(\tilde{l}_R) &= \kappa_L M_{1/2}^2 - \tfrac{1}{2}(1 - 4\sin^2\theta_W)\cos 2\beta m_Z^2 \end{aligned}$$

with $\kappa_L = 0.37$. The second relation follows from the hypothesis that the scalar masses are universal at the GUT scale, in particular $m^2(5^*) = m^2(10)$ within SU_5. This assumption can be tested by relating the mass difference between $\tilde{e}_L$ and $\tilde{e}_R$ to the SU_2 gaugino mass.

The typical results of an overall fit are illustrated in Table 2 [69].

In a much more difficult procedure the parameters may not only be fitted by assuming a universal set at the GUT scale from the start, but the set itself may be reconstructed by evolving the mass parameters from the electroweak scale to the unification scale [69]. This is the only way to reconstruct operationally the fundamental supersymmetric theory near the Planck scale from experimental observations at the electroweak scale.

Precision tests of supersymmetric particles in e^+e^- collider experiments can thus open a window to energy scales close to the Planck scale where gravity, the fourth of the fundamental forces, becomes an integral part of physics.

References

[1] S.L. Glashow, Nucl. Phys. 20 (1961) 579; S. Weinberg, Phys. Rev. Lett. 19 (1967) 1264; A. Salam, in Elementary Particle Theory, ed. N. Svartholm (Almqvist and Wiksells, Stockholm 1968).

[2] H. Fritzsch and M. Gell-Mann, Proc. XVI Int. Conf. on High Energy Physics, eds. J.D. Jackson and A. Roberts, eds, (Fermilab 1972).

[3] P.W. Higgs, Phys. Rev. Lett. 12 (1964) 132; Phys. Rev. 145 (1966) 1156; F. Englert and R. Brout, Phys. Rev. Lett. 13 (1964) 321; G.S. Guralnik, C.R. Hagen and T.W. Kibble, Phys. Rev. Lett. 13 (1964) 585.

[4] J.C. Pati and A. Salam, Phys. Rev. D10 (1974) 275; H. Georgi and S. Glashow, Phys. Rev. Lett. 32 (1974) 438; H. Fritzsch and P. Minkowski, An. Phys. 93 (1975) 193.

[5] J. Wess and B. Zumino, Nucl. Phys. B70 (1974) 39.

[6] E. Accomando et al., Phys. Rep. 299 (1998) 1, [hep–ph/9705442].

[7] H. Murayama and M.E. Peskin, Ann. Rev. Nucl. Part. Sci. 46 (1996) 553; P.M. Zerwas, Surv. High Energy Phys. 12 (1998) 209.

[8] F. Richard, Proceedings, LC Conference, Sitges 1999, [hep–ph/ 9909317].

[9] ATLAS Collaboration, Technical Design Report 1999; CMS Collaboration, Physics with CMS [www page].
[10] Prospective Study of Muon Storage Rings at CERN, B. Autin, A. Blondel and J. Ellis, eds, CERN 99–02; C.M. Ankenbrandt et al., Phys. Rev. ST Accel. Beams 2 (1999) 081001.
[11] F. Abe et al. [CDF Coll.], Phys. Rev. D50 (1994) 2966 and Phys. Rev. Lett. 74 (1995) 2626; S. Abachi et al. [D0 Coll.], Phys. Rev. Lett. 74 (1995) 2632.
[12] I.I. Bigi, Y.L. Dokshitzer, V. Khoze, J. Kühn and P.M. Zerwas, Phys. Lett. 181B (1986) 157.
[13] O. Podobrin, Proceedings, e^+e^- *Collisions at 500 GeV: The Physics Potential*, Munich–Annecy–Hamburg 1992/93, DESY 93–123C.
[14] J. Jersak, E. Laermann and P.M. Zerwas, Phys. Rev. D25 (1982) 363.
[15] M.E. Peskin and C. Schmidt, in Proceedings, *Physics and Experiments with* e^+e^- *Linear Colliders*, Saariselkä 1991, R. Orava, P. Eerola and M. Nordberg eds., World Scientific 1992.
[16] W. Bernreuther et al., in Proceedings, e^+e^- *Collisions at 500 GeV: The Physics Potential*, Munich–Annecy–Hamburg 1991/93, DESY 92–123A+B, 93–123C.
[17] V.S. Fadin and V.A. Khoze, JETP Lett. 46 (1987) 525 and Sov. J. Nucl. Phys. 48 (1988) 309; A.H. Hoang and T. Teubner, DESY 99–047, [hep–ph/9904468].
[18] P. Igo–Kemenes, M. Martinez, R. Miquel and S. Orteu, in Proceedings, e^+e^- *Collisions at 500 GeV: The Physics Potential*, Munich–Annecy–Hamburg 1991/93, DESY 92–123A+B, 93–123C.
[19] M. Martinez, Proceedings, LC Conference, Sitges 1999.
[20] K. Hagiwara, R.D. Peccei and D. Zeppenfeld, Nucl. Phys. B282 (1987) 253.
[21] B.W. Lee, C. Quigg and H.B. Thacker, Phys. Rev. Lett. 38 (1977) 883, and Phys. Rev. D16 (1977) 1519.
[22] R. Hawkings and K. Mönig, EPJdir. C *in prep.*, hep–ex/9910022.
[23] G. Wilson, Report at the DESY/ECFA LC Workshop, Strasbourg–Obernai 1999.
[24] S. Heinemeyer, T. Mannel and G. Weiglein, DESY 99–117, [hep–ph/ 9909538]; J. Erler, S. Heinemeyer, W. Hollik, G. Weiglein and P.M. Zerwas, DESY 99–177.
[25] K. Mönig, Report at the DESY/ECFA LC Workshop, Strasbourg–Obernai 1999.
[26] M. Veltman, Acta Phys. Polon. B8 (1977) 475.
[27] T. Appelquist and C. Bernard, Phys. Rev. D22, 200 (1980); A. Longhitano, Phys. Rev. D22, 1166 (1980); Nucl. Phys. B188, 118 (1981); T. Appelquist and G.-H. Wu, Phys. Rev. D48, 3235 (1993); M. Veltman, Report CERN 97–05.
[28] E. Boos, H.-J. He, W. Kilian, A. Pukhov, C.-P. Yuan and P.M. Zerwas, Phys. Rev. D57, 1553 (1998) and hep–ph/9908409.
[29] V. Barger, K. Cheung, T. Han and R.J. Phillips, Phys. Rev. D52 (1995) 3815.
[30] T. Barklow, in Proceedings, *Physics and Experiments with* e^+e^- *Linear Colliders*, Saariselkä 1991, R. Orava, P. Eerola and M. Nordberg eds., World Scientific 1992; D. Dominici, Riv. Nouv. Cim. 20 (1997) 1.
[31] A. Djouadi, Proceedings, *Workshop on Physics and Experiments with* e^+e^- *Linear Colliders*, Iwate 1995.
[32] A. Leike, Phys. Rep. 317 (1999) 143.
[33] N. Cabibbo, L. Maiani, G. Parisi and R. Petronzio, Nucl. Phys. B158 (1979) 295; M. Sher, Phys. Rep. 179 (1989) 273; M. Lindner, Z. Phys. C31 (1986) 295; J. Casas, J. Espinosa and M. Quiros, Phys. Lett. B342 (1995) 171; K. Riesselmann, DESY 97–222, [hep–ph/9711456].
[34] J. Ellis, M.K. Gaillard and D.V. Nanopoulos, Nucl. Phys. B106 (1976) 292; B.L. Ioffe and V.A. Khoze, Sov. J. Part. Nucl. 9 (1978) 50; B.W. Lee, C. Quigg and H.B. Thacker, Phys. Rev. D16 (1977) 1519.
[35] D.R.T. Jones and S.T. Petcov, Phys. Lett. B84 (1979) 440.
[36] P.M. Zerwas, Acta Phys. Pol. B30 (1999) 1871; M. Spira and P.M. Zerwas, Proceedings, 36. Int. Universitätswochen, Schladming 1997, hep–ph/9803257; C. Quigg, FERMILAB–CONF–99/033-T.
[37] A. Djouadi, M. Spira and P.M. Zerwas, Z. Phys. C70 (1996) 427.
[38] V. Barger, K. Cheung, A. Djouadi, B.A. Kniehl and P.M. Zerwas, Phys. Rev. D49 (1994) 79.
[39] W. Kilian, M. Krämer and P.M. Zerwas, Phys. Lett. B373 (1996) 135.
[40] P. Garcia–Abia and W. Lohmann, Proceedings, LC Conference, Sitges 1999, [hep–ex/9908065].

[41] P. Janot, in Proceedings, *Physics and Experiments with e^+e^- Linear Colliders*, Waikoloa/Hawaii 1993, F. Harris, S. Olsen, S. Pakvasa and X. Tata eds., World Scientific 1993.
[42] G. Borisov and F. Richard, Proceedings, LC Conference, Sitges 1999, hep–ph/9905413.
[43] M. Battaglia, *ibid.*, hep–ph/9910271.
[44] D. Reid, Report at the DESY/ECFA Workshop, Oxford 1999.
[45] W. Kilian, M. Mühlleitner and P.M. Zerwas, DESY 99–171.
[46] S. Yamashia, Proceedings, LC Conference, Sitges 1999.
[47] G. Jikia and S. Söldner–Rembold, Proceedings, LC Conference, Sitges 1999.
[48] A. Djouadi, J. Kalinowski and P.M. Zerwas, Z. Phys. C54 (1992) 255; S. Dawson and L. Reina, Phys. Rev. D59 (1999) 054012; S. Dittmaier, M. Krämer, Y. Liao, M. Spira and P.M. Zerwas, Phys. Lett. B 441 (1998) 383.
[49] A. Djouadi, W. Kilian, M. Mühlleitner and P.M. Zerwas, Eur. Phys. J. C10 (1999) 27.
[50] P. Lutz and P. Gay, Reports at the DESY/ECFA Workshops, Oxford/Strasbourg–Obernai 1999.
[51] J.F. Gunion and H.E. Haber, Nucl. Phys. B272 (1986) 1 and B278 (1986) 449.
[52] A. Djouadi, J. Kalinowski and P.M. Zerwas, Z. Phys. C57 (1993) 569; A. Djouadi, J. Kalinowski, P. Ohmann and P.M. Zerwas, Z. Phys. C74 (1997) 93.
[53] F. Zwirner, Proceedings, 36. Int. Universitätswochen, Schladming 1997.
[54] A.H. Chamseddine, R. Arnowitt and P. Nath, Phys. Rev. Lett. 49 (1982) 970; R. Barbieri, S. Ferrara and C.A. Savoy, Phys. Let. B119 (1982) 343.
[55] M. Dine, A. Nelson and Y. Shirman, Phys. Rev. D51 (1995) 1362; M. Dine, A. Nelson, Y. Nir and Y. Shirman, Phys. Rev. D53 (1996) 2658; G.F. Giudice and R. Rattazzi, CERN Report, hep–ph/9801271.
[56] G.F. Giudice, M.A. Luty, H. Murayama and R. Rattazzi, JHEP 9812 (1998) 027.
[57] J. Scherk and J.H. Schwarz, Nucl. Phys. B153 (1979) 61.
[58] J. Ellis, S. Kelley and D. V. Nanopoulos, Phys. Lett. 260B (1991) 131; U. Amaldi, W. de Boer and H. Fürstenau, Phys. Lett. 260B (1991) 447; P. Langacker and M. Luo, Phys. Rev. D44 (1991) 817.
[59] A. Bartl, W. Majerotto and B. Mösslacher in Proceedings, *e^+e^- Collisions at 500 GeV: The Physics Potential*, Munich–Annecy–Hamburg 1991/93, DESY 92–123A+B, 93–123C
[60] U. Martyn and G.A. Blair, hep–ph/9910416.
[61] S.Y. Choi, A. Djouadi, H. Dreiner, J. Kalinowski and P.M. Zerwas, Eur. Phys. J. C7 (1999) 123; S.Y. Choi, A. Djouadi, H.S. Song and P.M. Zerwas, Eur. Phys. J. C8 (1999) 669.
[62] T. Tsukamoto, K. Fujii, H. Murayama, M. Yamaguchi and Y. Okada, Phys. Rev. D51 (1995) 3153.
[63] G. Moortgat–Pick, H. Fraas, A. Bartl and W. Majerotto, Eur. Phys. C7 (1999) 113.
[64] See C. Heusch, ed, Proceedings, e^-e^- LC Conference Santa Cruz, Int. J. Mod. Phys. 11 (1996) 1.
[65] S. Kraml, Report at the DESY/ECFA Workshop, Oxford 1999.
[66] S. Ambrosanio and G.A. Blair, Eur. Phys. J. C in press, hep–ph/ 9905403.
[67] N. Arkani–Hamed, S. Dimopoulos and G. Dvali, Phys. Lett. B429 (1998) 263.
[68] See e.g. M.E. Peskin, Proceedings, LC Conference, Sitges 1999.
[69] G.A. Blair, W. Porod and P.M. Zerwas, DESY 99–181.